Reprinted from SPIE Vol. 192—Interferometry
© 1979 by the Society of Photo-Optical Instrumentation Engineers, Box 10, Bellingham, WA 98227-0010 USA

# Differential technique for accurately measuring the radius of curvature of long radius concave optical surfaces

**Mark C. Gerchman, George C. Hunter**
Zygo Corporation, Laurel Brook Road
Middlefield, Connecticut 06455

## Abstract

Described is a technique for accurately measuring the radius of curvature of very long radius concave optical surfaces in a relatively short working length. Presented is the basic theory of the technique and the detailed information necessary to provide for its practical application. Using the technique, radii of up to 175 meters can be measured to an accuracy of better than 0.01 percent with a one-meter long scale and slide, and in an overall working length of less than 5 meters. Generalizations of the technique allow for the measurement of convex surfaces and even longer radius concave surfaces. Photographs, interferograms, calculations, and an error analysis illustrate the technique.

## Introduction

The methods for measuring the radius of curvature of concave spherical optical surfaces are well known[1] and can be divided into two major categories: direct measurement methods in which the center of curvature is located and the distance between the surface and center of curvature is measured, and indirect measurement methods where the radius of curvature is calculated from a measurement of the sagitta of the surface. However, significant problems arise with either method when measuring very long radii. For example, direct measurement methods require large working distances and correspondingly long measuring transducers. With indirect methods, small errors in the sagitta measurement produce large errors in the calculated value of the radius.

The technique presented here provides a method for accurately calculating the radius of curvature of long radius concave optical surfaces by measuring differences in cavity lengths between successive-order confocal (retroreflecting) cavities formed by the surface under test and a plano reference surface.

## Description

In this differential measuring technique a cavity is formed between a plano surface and the concave surface whose radius we wish to measure. By varying the separation between surfaces we note that certain separations correspond to confocal cavity configurations (i.e., those configurations where collimated light entering the cavity through the plano surface is brought to a focus on one or the other of the surfaces). By measuring the distance traveled between any two successive confocal configurations we can calculate the radius of the concave surface. Because the separation between surfaces is greatly reduced in the higher order confocal configurations and the distance travelled between successive order configurations is smaller, surfaces with very long radii can be measured in short working spaces, using a correspondingly short measuring slide and transducer.

The successive orders of the confocal retroreflecting cavities are specified by a configuration number n. The n = 1 configuration is the standard plano-concave cavity where all rays incident normal from the plano surface reflect off the concave surface and come to focus on the plano surface (Fig. 1). The n = 2 configuration reduces the distance between the plano and concave surfaces so that all rays incident normal from the plano surface reflect off the concave surface, fold off the plano surface, and come to focus on the concave surface (Fig. 2). The n = 3 configuration further reduces the distance between the plano and concave surfaces so that all rays incident normal from the plano surface reflect off the concave surface, fold off the plano surface, again reflect off the concave surface, and come to focus on the plano surface (Fig. 3). Still higher order configurations add additional folds and reflections so that all odd order configurations focus the system on the plano surface and all even order configurations focus the system on the concave surface.

Though many standard optical techniques can be used to examine the confocal cavity for best focus, a particularly sensitive arrangement is to evaluate the cavity focus interferometrically. This can be accomplished by having the plano surface of the cavity be the beam splitting surface of the transmission element in a Fizeau interferometer.

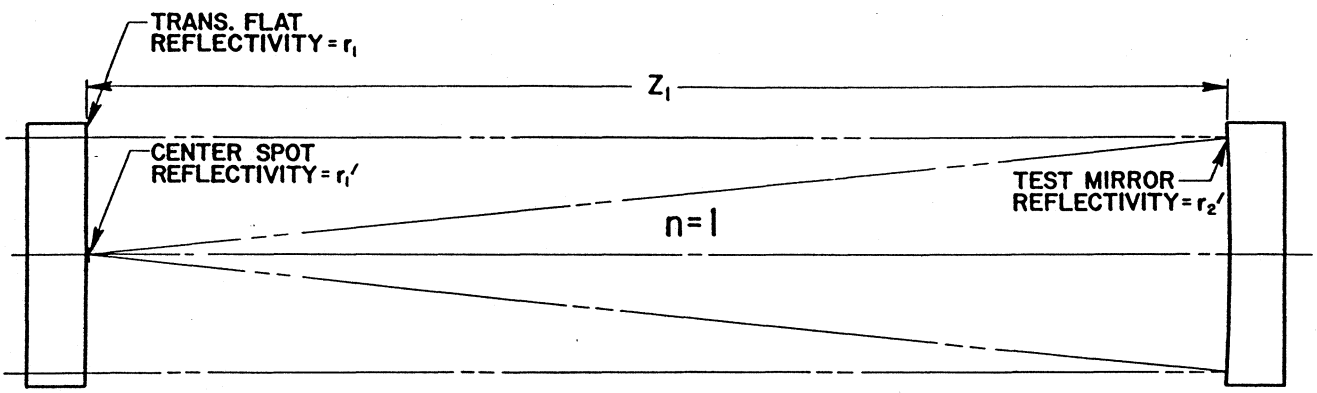


FIGURE 1

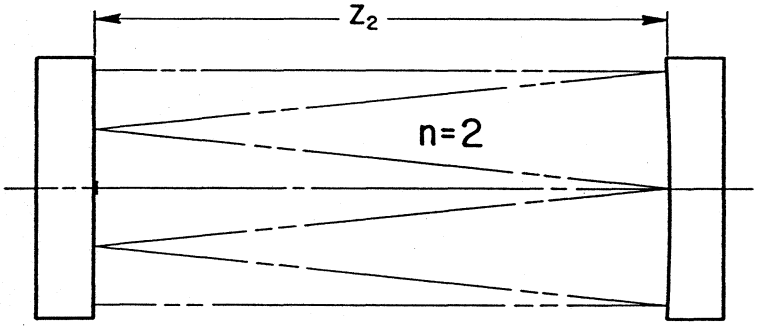


FIGURE 2

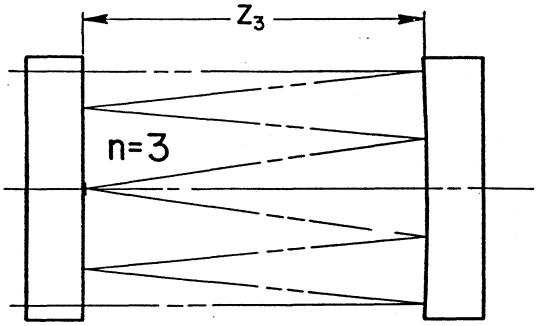


FIGURE 3

The technique can be generalized to provide for the measurement of convex surfaces by using a non-plano Fizeau transmission element in place of the plano element.

## Analysis

The equations that relate the cavity lengths, $z_n$, and the radius of curvature of the concave surface, R, as a function of the configuration number, n, are derived from a paraxial ray analysis. This is accomplished by repeated application of the Gaussian form of the image equation

$$2/R = 1/s_m + 1/s_m' , \tag{1}$$

and the conjugate recursion formula,

$$s_m = 2z_n - s'_{m-1}, \tag{2}$$

where m = k, k-1, k-2, ..., 0, and:

for n odd, k = (n-1)/2;

for n even, k = (n-2)/2.

An appropriate initial condition is determined for each configuration depending upon where the system comes to focus.

For n odd,

$$z_n = s_k' \tag{3}$$

For n even,

$$z_n = s_k'/2. \tag{4}$$

The analysis involves calculating the cavity length, $z_n$, in terms of the radius of curvature, R, and respective image and object conjugates, $s_m$ and $s_m'$, where each conjugate is calculated in terms of successive lower order conjugates. Beginning with the initial condition [Eq. (3) or Eq. (4)], the analysis continues relating cavity length to lower order conjugates until the final object conjugate, $s_o$, is reached. With the substitution that for a properly focused cavity the final object conjugate is infinity (i.e., $s_o = \infty$), the cavity length and radius are related by equations of the form,

$$z_n = C_n R. \tag{5}$$

The n = 3 configuration is evaluated to demonstrate the analysis (Fig. 4).

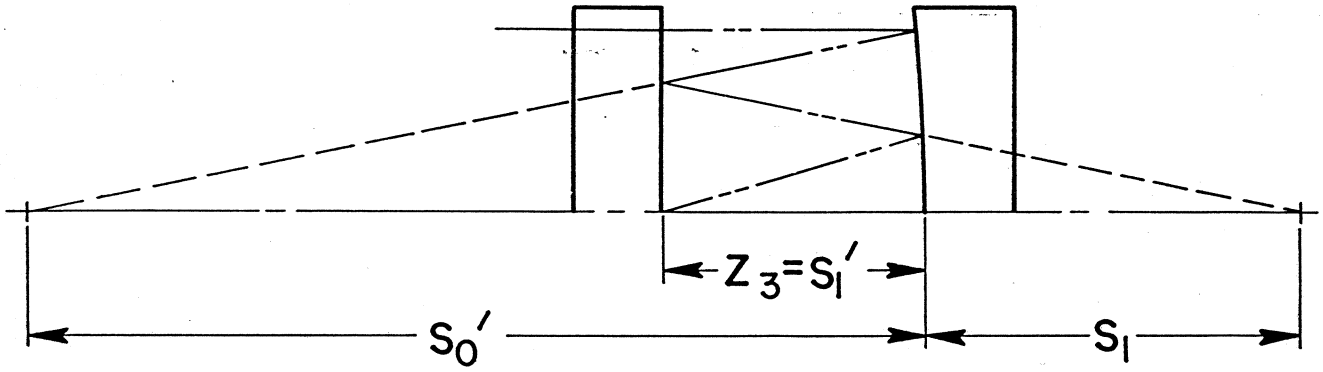


FIGURE 4

From Eq. (3) we have the appropriate initial condition, that is:

$$z_3 = s_1'. \tag{6}$$

By applying Eq. (1) and rearranging, we have the result,

$$s_1 = \frac{Rz_3}{2z_3 - R}. \tag{7}$$

Upon application of Eq. (2), the result is,

$$s_o' = 2z_3 - \frac{Rz_3}{2z_3 - R}. \tag{8}$$

Applying Eq. (1), again with the condition that $s_o = \infty$, yields upon substitution and rearrangement,

$$8z_3^2 - 8z_3R + R^2 = 0. \tag{9}$$

The solution of interest that gives the desired relationship is the root:

$$z_3 = 0.1464466R. \tag{10}$$

From Eq. (5), $C_n = 0.1464466$.

This procedure for deriving equations is valid for all configurations, although tedious in the higher order cases. Fortunately another means exists for obtaining these equations. Due to the specific form of the Gaussian image equation and the conjugate recursion formula, the odd configuration equations are identical to the even

order Chebyshev polynomials of the first kind, $T_{n+1}(x)$, (n=1,3,5...) where $x = z_n/R$. Similarly, the even configuration equations are identical to the even Chebyshev polynomials of the second kind, $U_n(x)$,(n=2,4,6...). This allows any order equation to be easily obtained from standard mathematical handbooks.[2] The solutions of interest are always the first positive root. The solutions for the first nine configurations are given in Table 1.

Table 2 expresses the relationships between the differences in cavity lengths between successive configurations, $z_n - z_{n+1}$, and the radius of curvature, R, of the surface under examination.

Table 1. Constants for relating cavity length to radius

$z_n = C_n R$

| n | $C_n$ |
|---|---|
| 1 | 0.5 |
| 2 | 0.25 |
| 3 | 0.1464466 |
| 4 | 0.0954915 |
| 5 | 0.0669873 |
| 6 | 0.0495156 |
| 7 | 0.0380603 |
| 8 | 0.0301537 |
| 9 | 0.0244717 |

Table 2. Equations for relating radius to differential cavity length

$R = 4 \quad (z_1 - z_2)$

$R = 9.65685 \quad (z_2 - z_3)$

$R = 19.62512 \quad (z_3 - z_4)$

$R = 35.08255 \quad (z_4 - z_5)$

$R = 57.23525 \quad (z_5 - z_6)$

$R = 87.29584 \quad (z_6 - z_7)$

$R = 126.47741 \quad (z_7 - z_8)$

$R = 175.99437 \quad (z_8 - z_9)$

## Error Analysis

The error sources that must be considered when using this technique are the same as those encountered with any direct measurement method. Mechanical errors are primarily associated with the measuring slide and transducer, while optical errors limit our ability to sense the position of best system focus.

The mechanical errors associated with the measuring slide and transducer are well understood and are covered in detail in other references.[3] However, because a much shorter slide and transducer are required when using this technique, the selection of these components with suitable accuracy is much less restrictive than with conventional methods.

In the following analysis we will evaluate the error in determining the position of best focus of the confocal cavity when using a Fizeau interferometer as the focus sensor.

Determination of the position of best focus of the interferometer cavity requires that we be able to detect small amounts of power (i.e., defocus) in the wavefront returning from the cavity. If the interferometer and interference cavity were perfect, the interference pattern would consist of straight, equally spaced fringes. Power in the return wavefront would appear as curvature of the fringes in the interference pattern and would be quite easy to evaluate. The evaluation of the amount of curvature of the fringes is complicated, however, by the presence of other aberrations. The interference pattern will, in general, be comatic in appearance due to the retroreflecting nature of the confocal cavity. In the retroreflecting cavity, the wavefront returning from the cavity is sheared rotationally by $180^{\circ}$ with respect to the reference wavefront. When this condition exists, any asymmetrical errors in the phase of the interferometer wavefront "print thru" and produce an interference pattern that is asymmetrical, or comatic, in nature. We can minimize the problem due to this aberration, however, by adjusting the plano transmission element in the interference cavity to optimize the orientation and spacing of the fringes. An orientation can be found for which the aberrations in the interference pattern are symmetrical about a straight central fringe and, once adjusted, the pattern will not change as we change the cavity configuration.

A second source of wavefront deformation is spherical aberration. Since we are primarily concerned with measuring very long radii (and consequently are working at very large f numbers), the amount of spherical aberration present is usually negligible. However, if the amount of spherical aberration present is significant, the optical path

difference due to the aberration can be measured in the interference pattern and the corresponding system focus error can be calculated and a correction can be made.[4]

The accuracy in evaluating the radius of curvature is related to the error in judging best cavity focus. The error in radius, dR, can be expressed as a function of the error in focus that produces an amount of power, w, in the wavefront returning from the system. The analysis from which this function is derived is based upon the recursion relationships already discussed. The analysis consists of relating the power in the return wavefront, w, to an error in the final image conjugate, $ds_o'$. This is then related to the error in cavity length, $dz_n$, and finally to the error in radius, dR.

Starting from the sagitta equation, we have,

$$w = R_w - (R_w^2 - a^2)^{1/2}, \tag{11}$$

where $R_w$ is the radius of the return wavefront and a is the radius of the limiting aperture of the system. For a system close to focus, $R_w >> a$, and the expression for the sagitta simplifies to,

$$w = a^2/2R_w. \tag{12}$$

From the Newtonian form of the image equation, $f^2 = xx'$, where the focal length, f, is R/2, the object distance, x, is $R_w$, and the image distance, x', is $ds_o'$. Substituting, we can write the error in the final image conjugate as

$$ds_o' = R^2/4R_w. \tag{13}$$

Substituting for $R_w$ from Eq. (12), Eq. (13) becomes,

$$ds_o' = wR^2/2a^2. \tag{14}$$

Defining the effective f number, F, as,

$$F = R/4a, \tag{15}$$

we obtain upon substitution the expression,

$$ds_o' = 8wF^2. \tag{16}$$

To calculate the error in cavity length, $dz_n$, as a function of the final image conjugate, $ds_o'$, we apply the Gaussian form of the image equation and the conjugate recursion formula as described previously. Because the analysis concludes at $ds_o'$ we can combine the two expressions into a single recursion relationship,

$$s'_{m-1} = 2z_n - \frac{s_m' R}{2s_m' - R}. \tag{17}$$

Taking the differential, we have,

$$ds'_{m-1} = 2dz_n + \frac{R^2}{(2s_m' - R)^2} ds_m'. \tag{18}$$

Applying this recursion relationship, with the same indices as used before, an expression for $ds_o'$ is obtained. When substituted into Eq. (16) we have for the error in cavity length, $dz_n$,

$$\text{for n odd,} \qquad dz_n = \frac{8wF^2}{(N_o')_n}; \tag{19}$$

$$\text{for n even,} \qquad dz_n = \frac{4wF^2}{(N_o')_n}. \tag{20}$$

The constants $(N_o')_n$ are evaluated by applying the following recursion equations.

For n odd:
$$N_{m-1} = 2 - N_m/(2C_nN_m-1); \quad (21)$$
$$N'_{m-1} = 2 + N'_m/(2C_nN_m-1)^2. \quad (22)$$

For n even:
$$N_{m-1} = 1 - N_m/(4C_nN_m-1); \quad (23)$$
$$N'_{m-1} = 1 + N'_m/(4C_nN_m-1)^2, \quad (24)$$

where $N_k = N'_k = 1$ and the $C_n$ values are obtained from Table 1. Grouping all the constants together, we can write the error in cavity length, $dz_n$, as a function of return wavefront power, w, and f number, F, as,

$$dz_n = C_n' wF^2, \quad (25)$$

where the values of $C_n'$ are given in Table 3.

Writing Eq. (5) in differential form, we have,

$$dz_n = C_n\, dR. \quad (26)$$

From Eqs. (25) and (26),

$$dR = (C_n'/C_n)wF^2, \quad (27)$$

where the values of $C_n'/C_n$ are given in Table 3.

Table 3. Constants for error analysis

| $dz_n=C_n' wF^2$ | | $dR=(C_n'/C_n)wF^2$ |
|---|---|---|
| n | $C_n'$ | $C_n'/C_n$ |
| 1 | 8. | 16. |
| 2 | 4. | 16. |
| 3 | 2. | 13.6569 |
| 4 | 1.105573 | 11.5777 |
| 5 | 0.666667 | 9.9521 |
| 6 | 0.432968 | 8.7441 |
| 7 | 0.292892 | 7.6955 |
| 8 | 0.207960 | 6.8967 |
| 9 | 0.152787 | 6.2434 |

The accuracy of the technique can be improved by two additional means. To more accurately determine the position of best focus, the cavity can be slightly defocused to both sides of best focus and a graph constructed of residual power in the wavefront versus slide position. From this plot the position of best focus can be more precisely located. Also, if more than one set of successive order configurations can be measured (e.g. n = 5 to 6 and n = 6 to 7), the measurements can be correlated and statistically averaged.

## Visibility Analysis

Visibility in the interference fringe pattern imposes a limit on the highest order of the test configuration that can be used. Because the first return reflection from the confocal cavity is of significantly higher intensity than any subsequent return reflections, we can consider the interference phenomena as being two beam in nature. Defining fringe visibility[5], V, for two beam interference in terms of the maximum and minimum intensity in the fringe pattern, we have,

$$V = (I_{max} - I_{min})/(I_{max} + I_{min}), \quad (28)$$

with,
$$I_{max} = I_1 + I_2 + 2(I_1I_2)^{1/2}, \quad (29)$$

and,

$$I_{min} = I_1 + I_2 - 2(I_1 I_2)^{1/2}, \tag{30}$$

where $I_1$ is the intensity of the reflection from the beamsplitter surface of the plano transmission element and $I_2$ is the intensity of the first return reflection from the confocal cavity (Fig. 5).

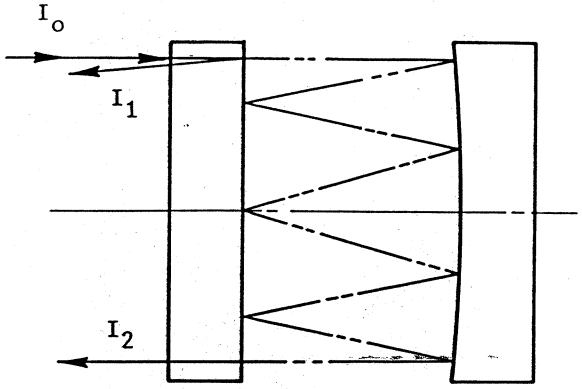


FIGURE 5

We can express the intensities, $I_1$ and $I_2$, in terms of the initial intensity, $I_o$ incident upon the beamsplitter surface through the transmission element and the reflectivities of the cavity surfaces (Fig. 1). Assuming no absorption, we have,

$$I_1 = r_1 I_o, \tag{31}$$

and:

for n = odd,

$$I_2 = (1 - r_1)^2 r_1^{n-1} r_1' r_2^{n+1} I_o ; \tag{32}$$

for n = even,

$$I_2 = (1 - r_1)^2 r_1^n r_2^{n+1} I_o ; \tag{33}$$

where $r_1$ is the reflectivity of the plano beamsplitter surface, $r_1'$ is the reflectivity of the small central focus area of the plano beamsplitter surface, and $r_2$ is the reflectivity of the concave test surface.

Upon substitution, Eq. (28) becomes:

for n = odd,

$$V = \frac{2[(1-r_1)^2 r_1^n r_1' r_2^{n+1}]^{1/2}}{r_1 + (1-r_1)^2 r_1^{n-1} r_1' r_2^{n+1}} ; \tag{34}$$

for n = even,

$$V = \frac{2[(1-r_1)^2 r_1^{n+1} r_2^{n+1}]^{1/2}}{r_1 + (1-r_1)^2 r_1^n r_2^{n+1}} . \tag{35}$$

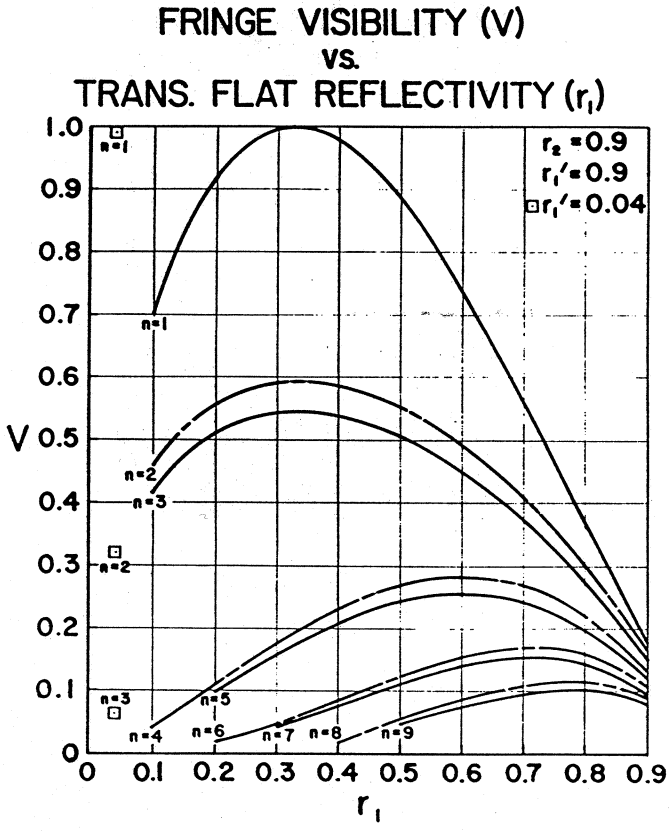


FIGURE 6

Figure 6 is a graph of visibility, V, as a function of the reflectivity of the plano beamsplitter surface, $r_1$, where the reflectivities of the central focus area and the concave test surface, $r_1$ and $r_2$, are 90 percent. Examples of interferograms with various visibilities are shown in Fig. 7. To optimize the visibility for higher order cavity configurations, it is evident from the graph that a relatively high reflectivity coating is required on the plano beamsplitter surface and a high reflectivity coating is required on the surface being measured. In practice, a beamsplitter with coating of 60 percent reflectivity and a central spot of 90 percent reflectivity provides workable fringe visibility up to the n = 9 order cavity configuration.

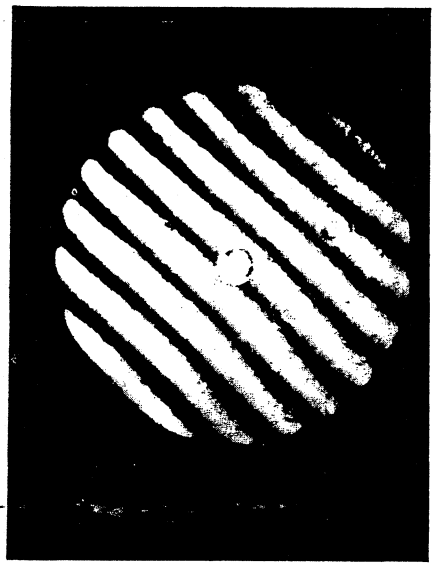

V = 0.42

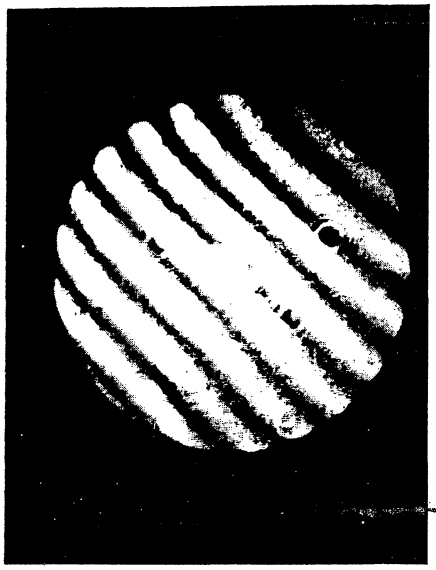

V = 0.28

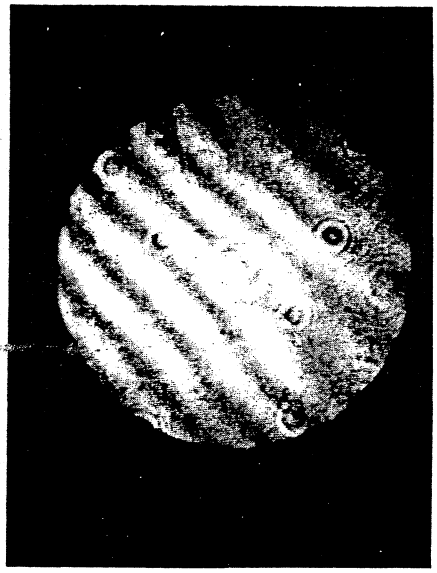

V = 0.17

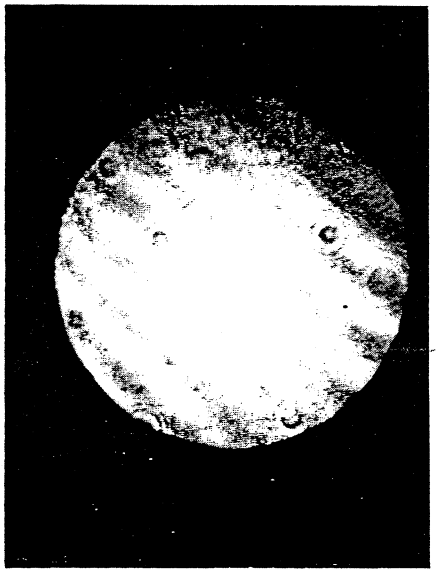

V = 0.08

FIGURE 6

## Application

To demonstrate the application of the technique, consider the following example. Assume we want to measure accurately the radius of curvature of a 200mm aperture concave surface whose nominal radius is 15 meters. To perform the measurement we have available a Fizeau interferometer with a 150mm aperture which is mounted on a table that provides a 1-meter long workspace as measured from the plano transmission element of the interferometer, and a suitably coated plano transmission element.

To determine which cavity configuration will fit in the workspace available, refer to Table 1. The lowest order configuration that we can use is the first one for which $z_n$ is less than 1 meter for R = 15 meters. From Eq. (5), $z_n = C_n R$, and we want $z_n/R$ to be less than 1/15 or 0.067. We therefore require a configuration for which $C_n$ is less than 0.067. The n = 6 configuration where $C_n = 0.0495156$ satisfies this requirement, so we can make our differential measurement between the n = 6 and n = 7 cavity configurations.

From Table 2, for the n = 6 to n = 7 case, R = 87.2958370 ($z_6$-$z_7$). For R = 15 meters $z_6$-$z_7$ = 171.829mm. We would, therefore, require a measuring slide and transducer with a 172mm range.

The accuracy of the measurement can be evaluated by calculating the error, dR, that would result from an error in locating the position of best focus of the confocal cavity. From Eq. (27), $dR = (C_n'/C_n)wF^2$. If we assume an error of 0.05λ (λ = 0.6328μm) in evaluating the power in the interference pattern, then $w = 0.3164 \times 10^{-4}$mm. From Eq. (15), F = R/4a, the f number can be calculated. For R = 15 meters and a = 75mm, F = 50. Note that the limiting aperture for this case is that of the interferometer. Table 3 provides the constants ($C_n'/C_n$). For n = 6, dR = 0.692mm and for n = 7, dR = 0.609mm. If we assume the worst case, where the errors add, the total error in the calculated radius is 1.301mm, or 0.0087 percent.

An additional error in the calculated value of the radius will enter due to errors in the measuring slide and transducer. Assume we can measure the position of the test piece to an accuracy of 10μm. The error in radius due to this error in position can be calculated using Eq. (26) and Table 1. From Table 1, $C_6$ = 0.0495156 and $C_7$ = 0.0380603. Substituting these values for $C_n$ and 10μm for $dz_n$ in Eq. (26), we have: for n = 6, dR = 0.202mm or 0.0013 percent, and for n = 7, dR = 0.263mm or 0.0018 percent. In the worst case, where all errors add, the total error in the calculated value of the radius for our example is 1.766mm or 0.0118 percent. If we make the more reasonable assumption that the errors add in a root sum square (RSS) fashion, the total error in the calculated value of the radius would be 0.980mm or 0.0065 percent.

If we repeat the above example for the n = 7 to n = 8 case, we see that the travel required for this measurement ($z_7$-$z_8$) is 118.599mm. The maximum error in the radius calculation for this case is 1.749mm, or 0.0117 percent, and the RSS error would be 0.921mm, or 0.0061 percent.

Performing both the $z_6$ to $z_7$ and $z_7$ to $z_8$ measurements would provide two values for the radius of curvature that can be averaged to improve the accuracy. Performing both measurements with a single setup would require a measuring slide and transducer with a 290 5mm range.

Figure 8 shows a test setup for performing radius measurements using the differential technique.

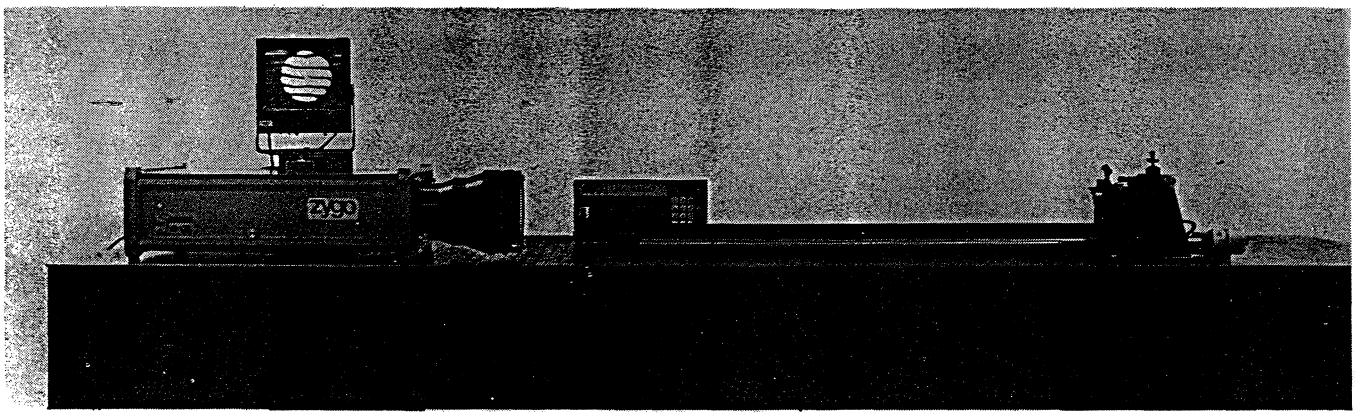


FIGURE 8

## Conclusion

The differential measuring technique provides a convenient method for measuring the radius of curvature of long radii concave optical surfaces. A short overall test setup, the requirement for a correspondingly short measuring slide and transducer, and high accuracy are the major advantages of the differential measuring technique. Accuracies of better than 0.01 percent can be achieved.

## Acknowledgments

The authors wish to express their appreciation to Ms Connie Carpentiere and Mr. Carl Bixby for assistance in the preparation of this manuscript.

## References

1. Malacara, Daniel, Optical Shop Testing, John Wiley and Sons, Inc. 1978.

2. Abramowitz, Milton and Stegon, Irene, Handbook of Mathematical Functions, National Bureau of Standards, Applied Mathematics Series 55, 1964.

3. Moore, Wayne R., Foundations of Mechanical Accuracy, Moore Special Tool Co. 1970.

4. Conrady, A. E., Applied Optics and Optical Design, Dover Publications, Inc., 1957.

5. Born, Max and Wolf, Emil, Principles of Optics, Pergamon Press, 1975.